Analytica Chimica Acta

Volume 985, 8 September 2017, Pages 202-212

Focusing and non-focusing modulation strategies for the improvement of on-line two-dimensional hydrophilic interaction chromatography × reversed phase profiling of complex food samples

Lidia Montero[a] Elena Ibáñez[a] Mariateresa Russo[b] Luca Rastrelli[c] Alejandro Cifuentes[a] Miguel Herrero[a]

https://doi.org/10.1016/j.aca.2017.07.013Get rights and content

Abstract

Comprehensive two-dimensional liquid chromatography (LC × LC) is ever gaining interest in food analysis, as often, food-related samples are too complex to be analyzed through one-dimensional approaches. The use of hydrophilic interaction chromatography (HILIC) combined with reversed phase (RP) separations has already been demonstrated as a very orthogonal combination, which allows attaining increased resolving power. However, this coupling encompasses different analytical challenges, mainly related to the important solvent strength mismatch between the two dimensions, besides those common to every LC × LC method. In the present contribution, different strategies are proposed and compared to further increase HILIC × RP method performance for the analysis of complex food samples, using licorice as a model sample. The influence of different parameters in non-focusing modulation methods based on sampling loops, as well as under focusing modulation, through the use of trapping columns in the interface and through active modulation procedures are studied in order to produce resolving power and sensitivity gains. Although the use of a dilution strategy using sampling loops as well as the highest possible first dimension sampling rate allowed significant improvements on resolution, focusing modulation produced significant gains also in peak capacity and sensitivity. Overall, the obtained results demonstrate the great applicability and potential that active modulation may have for the analysis of complex food samples, such as licorice, by HILIC × RP.

Keywords: Metabolite profiling, Two-dimensional LC, Licorice, Active modulation, Trapping columns, Resolution

1. Introduction

The use of multidimensional liquid chromatography (MDLC) within the food analysis field is gaining interest, as foods and food-related products are normally considered as very complex matrices [1]. Indeed, it is frequent to find food samples that are simply too complex to be analyzed by conventional one-dimensional chromatography. In other cases, food-related samples may not be so complex in terms of number of compounds present, but these could be composed by mixtures of closely related components that are also difficult to be resolved. Although there are several approaches to MDLC of food, the use of comprehensive two-dimensional liquid chromatography (LC × LC) coupled on-line, presents different advantages over off-line modes as well as over other couplings, such as heart-cutting two-dimensional LC. Most-notably, faster separations may be obtained with high resolving power in a fully-automated way, thus, increasing robustness and reproducibility [2], [3]. However, the optimization of a LC × LC method is far from being easy, as there are different inter-related parameters which modification may directly influence others [4]. These optimization challenges are even more pronounced when orthogonal separation mechanisms are coupled, which in practice, is the most-interesting approach. By selecting two independent non-correlated separation modes in both dimensions, significant gains on resolving power and peak capacity are potentially attainable. However, using two very different separation mechanisms in both dimensions means that important solvent incompatibility and/or immiscibility problems may be found. The combination between hydrophilic interaction chromatography (HILIC) in the first dimension (^{1}D) and reversed phase (RP) in the second dimension (^{2}D) has been shown to be characterized by a high degree of orthogonality for the analysis of complex food samples [5], providing with complementary retention. Although in

these two separation modes the same types of mobile phases are employed, their coupling can be termed as fairly incompatible, considering that the relative solvent strength is the opposite in each mode, thus, producing serious solvent mismatch.

In a LC × LC system, both dimensions are physically connected through the modulator. The most-widely employed modulator so far is based on the use of one or more switching valves equipped with two identical volume sampling loops [6]. This configuration allows the effective collection and injection of discrete ^{1}D effluent fractions into the ^{2}D continuously, by alternating the position and function of the two sampling loops. To translate this into practice, different analytical conditions should be established, mainly: i) a ^{1}D slow separation based on the use of very low flow rates, in order to minimize, as much as possible, the effluent fraction volume collected, and; ii) a fast ^{2}D using very high flow rates, in order to achieve fast separations in the shortest possible analysis time to allow a high ^{1}D sampling rate. As a consequence, set-ups involving the use of microbore columns in the ^{1}D combined with short wider columns (e.g., 4.6 mm i.d.) in the ^{2}D have provided good results [5]. This type of coupling implies the additional advantage of injecting relatively small volumes of ^{1}D effluent on the ^{2}D, thus, reducing possible band broadening. However, the main limitation directly related to the application of this approach is the characteristic low sensitivity obtained in LC × LC compared to regular one-dimensional methods, although potential deleterious issues due to solvent mismatch are significantly reduced [7].

To partially alleviate these problems, different modulators have been designed; among them, thermal modulators are included. Within this group, several improvements have been presented, such as a vacuum-assisted evaporation interface aimed to remove the solvent from the ^{1}D effluent prior transfer to the ^{2}D [8], or the development of an on-column thermal modulation device [9]. This latter device was shown to be able to apply heating and cooling cycles to capture and elute analytes to the ^{2}D producing narrower bands. However, due to their sophisticated and complicated design, these thermal modulators have not been to date extended to other applications. In parallel, new approaches have been explored taking advantage of the higher robustness and simplicity of valve-based modulation, such as the use of two parallel ^{2}D columns [10]. Another interesting possibility to enhance the performance is to substitute the regular sampling loops by trapping columns [10], [11], [12], [13]. By using this approach, analytes are adsorbed by the stationary phase of the trap, typically with similar selectivity to that found in the ^{2}D, during the collection position, and are then eluted by the ^{2}D mobile phase in the injection position. Although, theoretically, the injection in ^{2}D mobile phase could also help to produce narrow bands and even focusing at the top of the ^{2}D column, there still may exist solvent incompatibility issues that may imply that not all the analytes contained in the ^{1}D effluent are efficiently retained in the trap. To overcome this issue, a modulation procedure termed “active modulation” has recently been reported [14]; this approach is based on the introduction of a make-up flow of a weaker solvent after ^{1}D separation and before entrance to the trapping column. This way, a reduction in the solvent strength is fostered, increasing the retention of the trap towards the compounds separated in the ^{1}D. Subsequently, when the valve is actuated, those retained analytes can be eluted from the trap in narrow bands thanks to the ^{2}D mobile phase. From this basic procedure, other modifications can be performed in order not only to improve the transfer of ^{1}D effluent to the ^{2}D, but also to increase sensitivity and decrease analysis time. Although this active modulation approach retains a high potential for the analysis of complex samples, its applicability to food samples is still not sufficiently demonstrated.

For this reason, the goal of the present work is to explore new possibilities to improve the separation of complex food samples, looking for quantitative improvements on resolving power, avoiding ^{2}D band broadening, as well as on sensitivity, using licorice as model matrix. To this aim, different modifications at the modulator level are tested and compared, studying their applicability on a HILIC × RP coupling. The influence of the separation and modulation parameters applied on the separation and detection of the secondary metabolite profile of licorice, previously developed in our lab [15], including glycosylated flavanones and chalcones and other polyphenols as well as triterpene saponins, is evaluated.

2. Materials and methods

2.1. Samples and chemicals

Licorice samples (*Glycyrrhiza glabra*) from the region of Calabria, Italy, were collected in July 2015 and supplied from a local producer. For the extraction of secondary metabolites from this sample, a simple procedure based on solid-liquid extraction assisted by ultrasounds extraction was followed, as described before [16]. The extraction solvent was a binary mixture ethanol/water (1:1, v/v) using a sample-to-solvent ratio 1:5 (w/v) during 60 min. The resulting extract was filtered and evaporated to dryness. Prior injection, the extract was redissolved in water/acetonitrile (3:7, v/v).

HPLC grade ethanol and acetonitrile were purchased from VWR Chemicals (Barcelona, Spain) whereas ultrapure water was produced from a Milli-Q instrument (Millipore, Billerica, MA). Acetic and formic acids were supplied from Sigma-Aldrich (Madrid, Spain), while ammonium acetate was from Panreac (Barcelona, Spain).

2.2. Instrumentation

The LC × LC-DAD instrumentation consisted on a first dimension (^{1}D) composed by an Agilent 1200 series liquid chromatograph (Agilent Technologies, Santa Clara, CA) equipped with an autosampler. A Protecol flow-splitter (SGE Analytical Science, Milton Keynes, UK) was installed between the ^{1}D pumps and the autosampler in order to minimize the gradient delay volume of the pump and to obtain more reproducible low flow rates. The second dimension (^{2}D) was composed by an additional LC pump (Agilent 1290 Infinity). Both dimensions were connected by an electronically-controlled two-position ten-port switching valve (Rheodyne, Rohnert Park, CA, USA) acting as modulator equipped with two identical sampling loops or trap columns, as indicated. A diode array detector was coupled after the second dimension in order to register every ^{2}D analysis. The system was simultaneously controlled by two different PC running appropriate ChemStation software; one controlled the ^{1}D, the autosampler and DAD, whereas the other controlled the ^{2}D and actuated the switching valve. For the separations involving the use of a make-up flow, a third LC pump (Agilent 1200 Series) was connected through a t-piece between the outlet of ^{1}D and the switching valve. The used additional make-up flow was delivered at five-, seven- and nine-times the ^{1}D flow rate, as indicated.

The LC linear chromatograms were elaborated and visualized as 2D- and 3D-plots using LC Image software (version 1.0, Zoex Corp., Houston, TX).

2.3. HILIC × RP separation conditions

Different conditions and column combinations were employed during this research, as described in Section 3. The common analytical conditions for each column used in the ^{1}D were the following:

i) SeQuant ZIC-HILIC (150 × 1 mm, 3.5 μm, Merck, Darmstadt, Germany) column, eluted using (A) acetonitrile and (B) 10 mM ammonium acetate at pH 5.0 as mobile phases, according to the following gradient: 0 min, 3% B; 5 min, 3% B; 10 min, 5% B; 15 min, 10% B; 30 min, 20% B; 40 min, 20% B; 50 min, 30% B; 60 min, 30% B; 65 min, 40% B; 80 min, 40% B. The injection volume was 5 μL and the flow rate was set at 15 μL min^{-1}.

ii) ZIC-HILIC (250 × 2.1 mm, 3.5 μm, Merck, Darmstadt, Germany) column, eluted using (A) acetonitrile and (B) 10 mM ammonium acetate at pH 5.0 as mobile phases, according to the following gradient: 0 min, 3% B; 10 min, 3% B; 30 min, 10% B; 50 min, 15% B; 60 min, 20% B; 90 min, 40% B. The injection volume was 15 μL and the flow rate was set at 100 μL min^{-1}.

On the other hand, the common analytical conditions for each column used in the ^{2}D were the following:

i) Ascentis Express C_{18} (50 × 4.6 mm, 2.7 μm, Supelco, Bellefonte, CA) partially porous column using (A) water (0.1% formic acid) and (B) acetonitrile as mobile phases, eluted at 3 mL min^{-1} using two segment gradients: from 0 min to 23.4 min the ^{2}D gradient elution was 0 min, 0% B, 0.1 min, 5% B; 0.5 min, 35% B; 0.9 min, 70% B; 1 min, 90% B; 1.01 min, 0% B; 1.3 min, 0% B; from 23.4 to 80 min the employed gradient was

programmed as 0 min, 0% B; 0.1 min, 5% B; 0.3 min, 35% B; 0.5 min, 40% B; 0.9 min, 50% B; 1 min, 90% B; 1.01 min, 0% B; 1.3 min, 0% B.

ii) Ascentis Express C_{18} (30 × 4.6 mm, 2.7 μm, Supelco, Bellefonte, CA) partially porous column using (A) water (0.1% formic acid) and (B) acetonitrile as mobile phases, eluted at 2 mL min^{-1}. Different gradients were applied depending on the modulation time applied. The different step gradients are detailed in Table S1.

When indicated, sets of trapping columns formed by two identical cartridges were employed including C_{18} and phenyl-hexyl (10 × 3 mm, 2.6 μm, Accucore, Thermo Scientific, Waltham,MA) stationary phases.

UV-Vis spectra were collected in the range of 190–550 nm using a sampling rate of 20 Hz, while 254, 280 and 330 nm signals were also independently recorded.

2.4. Calculations

2.4.1. Peak capacity

Individual peak capacity for each dimension (n_c) was calculated according to eq. (1):(1)

where t_G is the gradient time and is the average peak width. For ^{1}D peak capacity calculations, the average peak width was obtained from *ca.* 10 representative peaks selected along the analysis. Likewise, for ^{2}D peak capacity, as much as possible peaks were considered (*ca.* 20 peaks, depending on the analysis). Additionally, ^1n_c was also calculated considering the peak broadening factor <β>, giving rise to a corrected ^{1}D peak capacity (eq. (2)), that considers the influence of the deleterious effect of undersampling. To estimate <β>, the sampling time (t_s) as well as the average width of ^{1}D peaks as standard deviation in time units ($^1\sigma$) before modulation were considered:(2)

For each two-dimensional set-up, different peak capacity values were estimated. First of all, theoretical peak capacity was obtained following the so-called product rule, using eq. (3), considering the individual peak capacities obtained in each dimension:(3)

As eq. (3) does not take into consideration the deleterious effects due to the modulation process as well as possible undersampling, a more realistic peak capacity value was obtained from the equation proposed by Li et al. [17], denominated here as practical peak capacity (eq. (4)):(4)

being ^2t_c, the ^{2}D separation cycle time, which is equal to the modulation time. This latter equation also includes the <β> parameter accounting for undersampling. Moreover, to more precisely compare among set-ups and in order to evaluate possible peak clusters along the 2D analysis and, thus, to estimate 2D space coverage, the orthogonality degree (A_O) was considered to offer the denominated 2D corrected (also known as effective) peak capacity, as follows:(5)

2.4.2. Orthogonality

Among the different approaches that have been described and published to quantify the orthogonality degree of a two-dimensional set-up [18], the method proposed by Camenzuli and Schoenmakers [19] was employed in the present work to calculate system orthogonality (A_O). This procedure takes into account the spread of each peak along the four imaginary lines that cross the 2D space forming an asterisk, that is Z_1, Z_2 (vertical and horizontal lines) and Z_-, Z_+ (diagonal lines of the asterisk). Z parameters describe the use of the separation space with respect to the corresponding Z line, allowing to semi-quantitatively diagnose areas of the separation space where sample components are clustered, thus, reducing in practice orthogonality. For the determination of each Z parameter, the S_{Zx} value was calculated, as the measure of spreading around the Z_x line, using the retention times of all the separated peaks in each 2D analysis.

2.4.3. Two-dimensional resolution

The resolution metric for two-dimensional separations proposed by Peters et al. [20] was employed to calculate a representative resolution value and the separation quality of each set-up. This measure is based on the valley-to-peak ratio between two neighbor peaks. To establish the valley-to-peak ratio between two peaks (peak 1 and peak 2), three maximum intensities are considered: the maximum of

the peak 1 (max1), the saddle point between both peaks (S) and the maximum of peak 2 (max2), as well as the distances between max1 and S, $d_{1,S,}$ and the distance between S and max2, $d_{S,2}$.(6)
(7)
where $\Delta^1 t_{R1,S}$ and $\Delta^2 t_{R1,S}$ are the differences on time between max1 and S in the ^{1}D and ^{2}D and $\Delta^1 t_{RS,2}$ and $\Delta^2 t_{RS,2}$ the difference between S and max2 in both dimensions.
Then, the intensity g is defined in accordance with the graphic showed in Fig. S1. Intensity g is calculated by:(8)
where h_{max1} and h_{max2} are the maximum intensities of peak 1 and peak 2, respectively.
The valley-to-peak ratio (V) is calculated as:(9)
Finally, resolution (Rs) is estimated by the following equation:(10)
In this work, the resolution measurement of two target critical pairs of peaks was calculated in each instrumental configuration, and results obtained compared among them.

3. Results and discussion

In our previous work, the first LC × LC application devoted to the profiling of secondary metabolites in licorice was developed [15]. Although the method was characterized by excellent separation capabilities, being possible to detect around 80 compounds from different metabolite families in just one sample, further optimization is desirable to increase sensitivity and to further improve performance. This is mainly interesting due to the fact that this sample is a very diverse and complex mixture of some closely related components, such as glycosylated flavanones and chalcones among other polyphenols as well as triterpene saponins. In the present work, we have applied several strategies, using licorice as a model complex real food sample in order to quantitatively evaluate the attainable performance by introducing new changes in the interface.

3.1. Non-focusing modulation

3.1.1. Influence of transfer volume/fraction solvent

The most-extended approach to interface both dimensions in LC × LC is the use of two identical sampling loops installed on the switching valve(s) acting as modulator. In our original method, two 30 μL sampling loops were employed with satisfactory results. However, modifications at the interface and columns combination levels could further improve two of the most important points in a comprehensive LC separation: ^{1}D undersampling and ^{2}D band broadening. These two parameters have a clear deleterious effect both on the resolving power as well as on the attainable peak capacity, and thus, should be minimized. The coupling between HILIC and RP is characterized by a very good degree of orthogonality, thus, being very attractive for the analysis of complex samples. Nevertheless, it generates a solvent mismatch during the transfer of ^{1}D effluent, considering that the weaker solvent in the ^{1}D is the stronger one on the ^{2}D environment. According to the intensity of this issue, the resulting ^{2}D separations may be completely ruined, or just worsened to a certain degree depending on the extent of the associated band broadening effect. For this reason, one of the possible strategies to avoid or reduce the mentioned solvent strength mismatch is to dilute the ^{1}D effluent before its transfer to the ^{2}D. When using a non-focusing modulation procedure based on sampling loops, this effect may be obtained through the use of loops with an internal volume higher than the strictly required to collect the ^{1}D effluent during the length of a modulation. That way, ^{1}D effluent supposes only part of the available loop volume whereas the rest is filled with ^{2}D starting mobile phase. However, it has to be also considered that, since short columns are employed in the ^{2}D to obtain fast separations, the increase on the sampling loop volume, which is also the injection volume for each individual ^{2}D separation, may negatively influence the separation [21].
Accordingly, the first step was to study the effects of sampling volume and fraction solvent on the ^{2}D, comparing the separation attainable using sampling loops with different internal volume, i.e., 20, 30 and 50 μL, operated in forward elution. To do that, experimental conditions based on the use of the ZIC-HILIC microbore column in the ^{1}D and the use of a 50 × 4.6 mm, 2.7 μm C_{18} partially porous

column in the ^{2}D, using 78 s as modulation and ^{2}D analysis time, were applied (see Section 2.3). As can be observed in Table 1 and Figs. S2A–C, the results in terms of overall separation, resolution and orthogonality were fairly similar. Interestingly, a slight but noticeable increase on theoretical peak capacity was obtained when the sampling loops volume was bigger. This trend would correspond to a decrease on average ^{2}D peak widths as a result of higher dilution of the ^{1}D effluent and, thus, to the injection of each fraction on a weaker solvent, which helps to improve peak shapes with respect to less diluted fractions. As can be also observed in Table 1, 50 μL fractions injected in the ^{2}D meant an injection volume of 10% of column void volume, considering that partially porous particles may occupy around 40% of the total available column inner volume [22], [23]. Thus, the reduction on the fraction solvent strength obtained when using 50 μL sampling loops (a 2.6-fold dilution) was able to make up for the possible deleterious effect due to increased injection volume. In fact, the use of 10% column void volume was significantly higher than the 3% previously reported in order to not get peak distortion [21]. In spite of the increment obtained in theoretical peak capacity, no practical gains on separation were observed (Figs. S2A–C).

Table 1. Comprehensive two-dimensional method parameters applied to the profiling of secondary metabolites from licorice using non-focusing modulation.

		^{2}D - C_{18} 50 × 4.6 mm, 2.7 μm			^{2}D - C_{18} 30 × 4.6 mm, 2.7 μm		
	Sampling loop volume	**20 μL**	**30 μL**	**50 μL**	**20 μL**	**30 μL**	**50 μL**
^{1}D	L (mm)	150	150	150	150	150	150
	I.D. (mm)	1.0	1.0	1.0	1.0	1.0	1.0
	Particle size (μm)	3.5	3.5	3.5	3.5	3.5	3.5
	Flow rate (μL min^{-1})	15	15	15	15	15	15
(min)	2.69 2.69 2.69	2.47 2.47	2.47				
$^{1}n_c$	30 30 30	33 33	33				
<β>	1.33 1.33 1.33	1.25 1.25	1.25				
$^{1}n_c$ corr.	23 23 23	27 27	27				
^{2}D							
(s)	1.06	0.90	0.78	1.02	1.00	1.00	
$^{2}n_c$	75	88	101	60	61	61	
LC × LC	Analysis time (min)	80	80	80	80	80	80
	t_s	1.93σ	1.93σ	1.93σ	1.62σ	1.62σ	1.62σ
	Modulation time (min)	1.3	1.3	1.3	1.0	1.0	1.0
	M – number of modulations	62	62	62	80	80	80
	$^{2}V_{inj}$ (V dilution)	20 μL (0.5 μL)	30 μL (10.5 μL)	50 μL (30.5 μL)	20 μL (5.0 μL)	30 μL (15.0 μL)	50 μL (35.0 μL)
	% ^{2}D column void volume	4%	6%	10%	7%	10%	17%
	Gradient delay volume (mL)	0.72	0.74	0.76	0.48	0.48	0.51
	^{2}D column operation preassure (bar)	299	295	298	187	185	190
	Z_1	0.84	0.91	0.92	0.89	0.82	0.85
	Z_2	0.97	0.96	0.99	0.97	0.98	0.97
	Z_-	0.69	0.77	0.81	0.91	0.89	0.86
	Z_+	0.83	0.87	0.84	0.99	0.95	0.99
	A_O	68%	76%	79%	82%	82%	84%
	Resolution pair 1	0.65	0.67	0.70	0.75	0.83	0.89
	Resolution pair 2	–	–	–	–	–	–
	Normalized sensitivity	0.85	1.00	1.37	1.08	1.32	1.61
	$^{2D}n_c$ theoretical	2250	2640	3030	1980	2013	2013
	$^{2D}n_c$ practical	1730	1964	2253	1706	1736	1780

$^{2D}n_c$ corr.	1401	1493	1780	1399	1424	1495

<β>, average ^{1}D broadening factor; $^{1}n_c$ corr.: calculated according to eq. (2); t_s, sampling time; A_O, orthogonality; $^{2D}n_c$ theoretical: $^{1}n_c \times {}^{2}n_c$; $^{2D}n_c$ practical: calculated according to eq. (4); $^{2D}n_c$ corr.: $^{2D}n_c \times A_0$.

3.1.2. Influence of sampling frequency

Possible enhancements on resolving power could be obtained minimizing the effect of ^{1}D undersampling. One of the concepts that characterize the performance of an on-line LC × LC method is the importance of maintaining the separation obtained in the ^{1}D during the transfer of ^{1}D effluent to the ^{2}D. If the sampling process is too slow to collect fractions where two well separated ^{1}D peaks are involved, undersampling arises; in that case, a remix of these previously separated peaks occurs in the transfer process, producing a loss of the ^{1}D separation and peak capacity. To reduce this negative effect, higher sampling frequencies should be applied, in order to obtain more ^{1}D fractions analyzed in the ^{2}D. Murphy et al. [24] established the widely-accepted rule of sampling 3–4 times each ^{1}D peak to solve the remix problem and to maintain the ^{1}D separation. However, in this case, due to instrumental limitations on maximum bearable backpressure, it was not possible to reduce the analysis time used with the 50 mm C_{18} partially porous column employed. Changes in the ^{2}D gradient did not produce any noticeable improvement either. For this reason, an even shorter column was tested. A 30 × 4.6 mm C_{18} partially porous column (2.7 μm) was coupled to the formerly optimized ^{1}D. By using this shorter column, a proper separation was obtained allowing a decrease on total ^{2}D analysis time (gradient time + re-equilibration time) to just 60 s. Under these analytical conditions, the use of the three different transfer volumes was studied (Figs. S2D–F). As can be observed from the data summarized in Table 1, theoretical peak capacities obtained using the 30 mm column were lower than those attainable using the 50 mm, as a result of the great dependence of $^{2}n_c$ on the available gradient time. However, as a result of the faster ^{1}D sampling rate applied when the shorter column was used, both orthogonality and resolution of pair 1 were improved, independently of the transfer volume employed (see Table 1). This improvement was more pronounced when using 50 μL sampling loops, as deduced from the data shown on Table 1 and illustrated in Fig. 1A–B and Fig. S2. In this latter set-up, the ^{2}D injection volume was equal to 17% of column void volume. Although this relative injection volume is rather high, no appreciable distorted peaks were detected compared to 20 and 30 μL transfer volumes; indeed, the dilution effect achieved using 50 μL, again allowed better retention of compounds due to the greater dilution in ^{2}D compatible mobile phase could produce a better interaction of the analytes with the stationary phase (see Figs. S2D–F and Fig. S3).

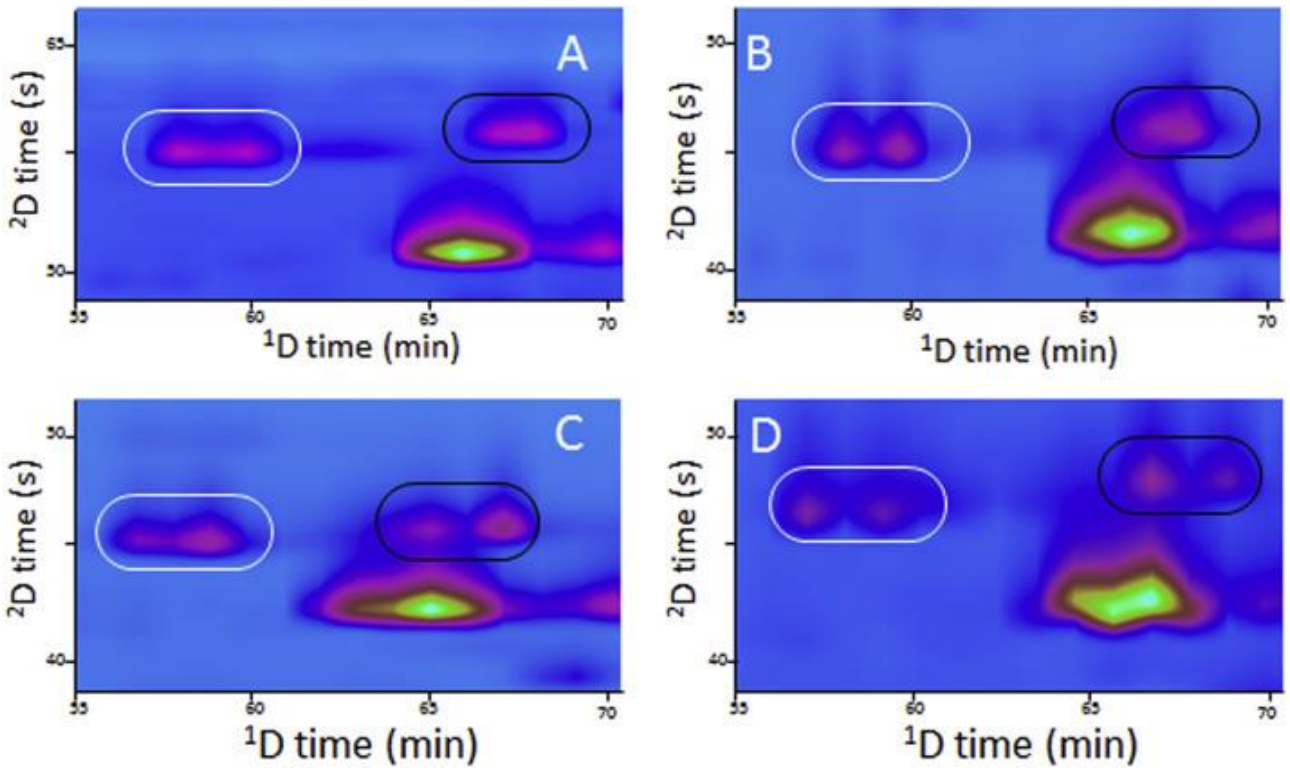

Fig. 1. Resolution obtained for peaks included in critical pair 1 (white oval) and in critical pair 2 (black oval) in the different set-ups studied. A, using 50 μL sampling loops in combination with a 50 mm long column in the ^{2}D; B, using 50 μL sampling loops in combination with a 30 mm long column in the ^{2}D; C, using Phenyl-hexyl trapping columns with forward elution, and; D, using active modulation with phenyl-hexyl traps and make-up flow rate equal to 9-times ^{1}D flow rate.

Although these conditions clearly improved the results attainable using the longer column, the use of higher separation temperature was also explored to investigate if proper ^{2}D separations could be obtained in even shorter analysis times, thus, further increasing ^{1}D sampling rate. To do that, the ^{2}D column was thermostated at 40 °C and several changes were applied to the gradient profile to adapt the separation to a total 39 and 50 s analysis times (Table S1). In order to establish a wider evaluation, the results obtained using the different mentioned modulation times (39, 50 and 60 s) were also compared with the longer 78 s ^{2}D modulation time previously employed with the 50 mm column. In this regard, considering that faster ^{1}D sampling rates imply that less ^{1}D effluent volume is transferred to the ^{2}D, the use of sampling loops volume of 50 μL was considered too high; for this reason, to perform these series of experiments, 20 μL sampling loops were installed in the switching valve, allowing more discrete transfers equivalent to 7% of total ^{2}D column void volume. Results are summarized in Table S2 and Fig. 2. As can be observed, as the modulation time was reduced, $^{2}n_{c}$ values also decreased, as a result of the great influence that this value retains from the available ^{2}D t_{G}. In consequence, the practical 2D peak capacity also tended to decrease. However, the observed decrease is not more pronounced thanks to the better peak shapes obtained as a result of a steeper gradient slope and higher dilution effect when using 39 s as modulation time; at those conditions, just 9.5 μL of ^{1}D effluent were transferred in each modulation, whereas the rest of the sampling volume was filled with ^{2}D mobile phase, thus, helping to reduce the solvent strength mismatch. Moreover, the effect of higher sampling rate is also illustrated on the attainable resolution between the two pairs of compounds studied. As illustrated in Fig. 2, resolution between pair 1 improved when reducing the modulation time. In addition, compounds in pair 2 remained coeluted using modulation times of 78 and 60 s, but they could be separated using shorter modulation times.

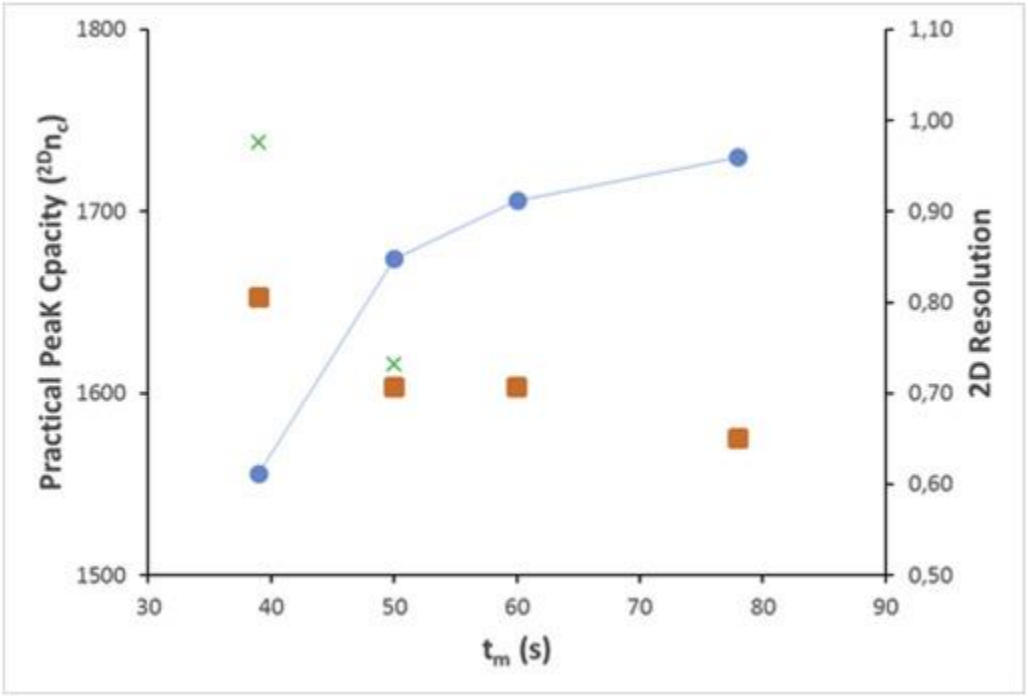

Fig. 2. Dependence of practical peak capacity ($^{2D}n_{c,practical}$) (●), 2D resolution reached for pair 1 (■), and 2D resolution for pair 2 (×) on modulation time. For detailed separation conditions, see section 2.3.

3.2. Focusing modulation using trapping columns

One of the possible implementations to reduce ^{2}D band broadening and to increase sensitivity limiting dilution is the use of trapping columns in the valve-based modulator. Reduction on band broadening is accomplished by introducing a focusing effect, considering that the analytes eluting from the ^{1}D would be entrapped in the trapping column during the collection position. Once the valve is actuated, ^{2}D mobile phase would desorb the analytes in discrete bands, injecting them into the ^{2}D column. Even if this approach has a good potential, its use is very limited compared to regular loops-based modulation. In the food analysis field, only C_{18} trapping columns have been reported [10], [25], in order to exactly match the selectivity of the ^{2}D column. In the present work, the use of trapping columns-based modulation to increase resolving power and sensitivity is extended to other stationary phases. Namely, the use of C_{18} and phenyl-hexyl trapping columns have been explored. The traps (10 × 3.0 mm, 2.6 μm) were installed in the modulator using the minimum possible extra volume for connections. The trapping columns void volume was 42 μL. Moreover, two elution configurations were compared, namely, forward and backflush elution. The use of the shortest available ^{2}D column was maintained, setting a modulation time of 60 s. Table 2 reports the most important method parameters related to these analyses. As can be observed, very similar results could be obtained using the two stationary phases available as well as both elution modes in terms of peak capacity and orthogonality attainable. Interestingly, using both elution modes resolution of critical pair 1 was maintained with respect to the best value attainable using non-focusing modulation, whereas, pair 2, that coeluted using the same separation conditions (60 s modulation time) with sampling loops, was also resolved. In any case, forward elution produced better resolution results for both tested stationary phases. Moreover, as can be appreciated from Fig. S4, in general, ^{2}D peak shapes were improved also under forward elution compared to backflush elution. This effect would be obtained as a result of the longer available interaction allowed under forward elution, bearing in mind that the trapping column was not fully filled with ^{1}D effluent during the collection position (see Fig. 3A and B). In addition, although reduced to a minimum, a 2 μL tube was necessary to connect the trapping columns to the valve; consequently, there was a small fraction of ^{1}D effluent that did not enter the trapping column when backflush elution was employed (Fig. 3B).

Table 2. Comprehensive two-dimensional method parameters applied to the profiling of secondary metabolites from licorice using trapping columns-based focusing modulation.

				Forward elution		**Backflush elution**		
	Trapping column			**C18**	**Phenyl-hexyl**	**C18**	**Phenyl-hexyl**	
^{1}D	L (mm)			150	150	150	150	
	I.D. (mm)			1.0	1.0	1.0	1.0	
	Particle size (μm)			3.5	3.5	3.5	3.5	
	Flow rate (μLmin^{-1})			15	15	15	15	
(min)	2.11	2.11	2.11	2.11				
$^{1}n_c$	39	39	39	39				
<β>	1.32	1.32	1.32	1.32				
$^{1}n_c$ corr.	30	30	30	30				
^{2}D								
(s)	0.97				0.96	0.98	0.98	
$^{2}n_c$	63				64	62	62	
	Analysis time (min)				80	80	80	80
	t_s				1.88σ	1.88σ	1.88σ	1.88 σ
	Modulation time (min)				1.0	1.0	1.0	1.0
	M – number of modulations				80	80	80	80
	Gradient delay volume (mL)				0.51	0.51	0.44	0.44
	^{2}D column operation preassure (bar)				260	258	253	254
LC × LC	Z_1				0.94	0.86	0.83	0.87
	Z_2				0.92	0.94	0.97	0.93
	Z_-				0.94	0.89	0.92	0.97
	Z_+				0.93	0.98	0.92	0.83
	A_0				87%	84%	83%	81%
	Resolution pair 1				0.80	0.80	0.79	0.81
	Resolution pair 2				0.81	0.85	0.72	0.78
	Normalized sensitivity				1.15	0.99	0.59	0.75
	$^{2D}n_c$ theoretical				2457	2496	2418	2418
	$^{2D}n_c$ practical				1792	1811	1777	1777
	$^{2D}n_c$ corr.				1559	1521	1475	1439

<β>, average ^{1}D peak broadening factor; $^{1}n_c$ corr.: calculated according to eq. (2); t_s, sampling time; A_O, orthogonality; $^{2D}n_c$ theoretical: $^{1}n_c \times {}^{2}n_c$; $^{2D}n_c$ practical: calculated according to eq. (4); $^{2D}n_c$ corr.: $^{2D}n_c \times A_O$.

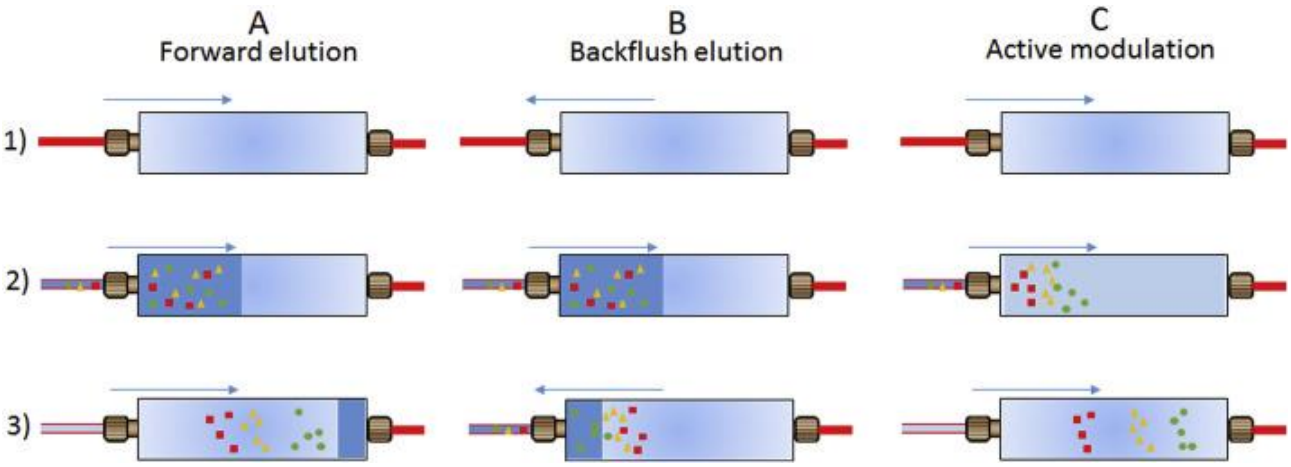

Fig. 3. Hypothetical scheme of the retention/elution of secondary metabolites from licorice into the trapping columns under forward elution mode (A), backflush elution mode (B), and active modulation (C) set-ups studied, following the procedure: 1) Trapping column filled with ^{2}D initial mobile phase (injection position, just after valve actuation); 2) Trapping column filled with ^{1}D effluent fraction (collection position) diluted in strong (A and B) or weak (C) solvent; 3) start of ^{2}D gradient. Arrows indicate flow direction.

3.3. Focusing using active modulation

The use of active modulation is a further evolution of the direct use of trapping columns. This modulation procedure, recently proposed [13], is based on the use of an additional make-up flow of a weak solvent for the ^{2}D in order to reduce the strength of the ^{1}D effluent prior entering the trapping column. This way, the interaction between the analytes and the functional groups in the trap is fostered, as illustrated in Fig. 3C. Therefore, considering the high potential and relative simplicity that this implementation may have, it is worth to study its application to complex food samples. Considering the ^{1}D and ^{2}D mobile phases compositions, it was decided to use ultrapure water (0.1% formic acid) as make-up flow. It has been previously observed that a flow rate for the additional make-up flow 7-times higher than the ^{1}D flow rate was appropriate to achieve the desired effect [13]. However, to further study the possible influence of make-up flow rate on the overall separation performance, three different flow rates for each set of trapping columns (C_{18} and phenyl-hexyl) were tested, i.e., 5-, 7- and 9-times the ^{1}D flow rate. Table 3 summarizes the data describing the performance attained using active modulation for the profiling of secondary metabolites in licorice. As can be appreciated, as for trapping columns, the performance attainable using both stationary phases was very similar. In both cases, the use of higher make-up flow rates allowed a slight improvement on peak capacity, whereas orthogonality values were essentially maintained. More relevant was the improvement observed for the resolution between the two studied pairs; in this regard, the use of make-up flow rates 9-times higher than the ^{1}D flow rate produced the best results (Fig. 4).

Table 3. Instrumental parameters employed and method performance descriptors from the use of active modulation for the profiling of secondary metabolites from licorice.

		C18 trapping columns			Phenyl-hexyl trapping columns		
	Make-up flow rate	**5 × ^{1}F**	**7 × ^{1}F**	**9 × ^{1}F**	**5 × ^{1}F**	**7 × ^{1}F**	**9 × ^{1}F**
^{1}D	L (mm)	150	150	150	150	150	150
	I.D. (mm)	1.0	1.0	1.0	1.0	1.0	1.0
	Particle size (μm)	3.5	3.5	3.5	3.5	3.5	3.5
	^{1}F (Flow rate, μL min^{-1})	15	15	15	15	15	15
(min)		2.11	2.11	2.11	2.11	2.11	2.11
^1n_c		39	39	39	39	39	39
<β>		1.33	1.33	1.33	1.32	1.32	1.32
^1n_c corr.		29	29	29	30	30	30
^{2}D							
(s)		0.93			0.84	0.81	0.96	0.84	0.81	
^2n_c		66			73	75	63	73	75	
	Analysis time (min)				80	80	80	80	80	80
	t_s				1.88σ	1.88σ	1.88σ	1.88σ	1.88σ	1.88σ
	Modulation time (min)				1.0	1.0	1.0	1.0	1.0	1.0
	M – number of modulations				80	80	80	80	80	80
	Gradient delay volume (mL)				0.49	0.49	0.49	0.49	0.49	0.49
	Column operation preassure (bar)				266	267	266	259	261	262
	Z_1				0.87	0.89	0.90	0.87	0.87	0.88
	Z_2				0.98	0.96	0.96	0.96	0.94	0.94
LC × LC	Z_-				0.91	0.92	0.91	0.87	0.89	0.89
	Z_+				0.93	0.93	0.94	0.96	0.97	0.95
	A_O				85%	86%	86%	84%	84%	84%
	Resolution pair 1				0.69	0.82	0.85	0.71	0.91	0.93
	Resolution pair 2				0.81	0.86	0.88	0.82	0.86	0.88
	Normalized sensitivity				1.46	1.59	1.98	0.91	1.67	2.01
	$^{2D}n_c$ theoretical				2574	2847	2925	2457	2847	2925
	$^{2D}n_c$ practical				1888	2075	2128	1806	2070	2131
	$^{2D}n_c$ corr.				1605	1785	1830	1517	1739	1790

<β>, average ^{1}D peak broadening factor; ^1n_c corr.: calculated according to eq. (2); t_s, sampling time; A_O, orthogonality; $^{2D}n_c$ theoretical: $^1n_c \times {}^2n_c$; $^{2D}n_c$ practical: calculated according to eq. (4); $^{2D}n_c$ corr.: $^{2D}\, n_c \times A_O$.

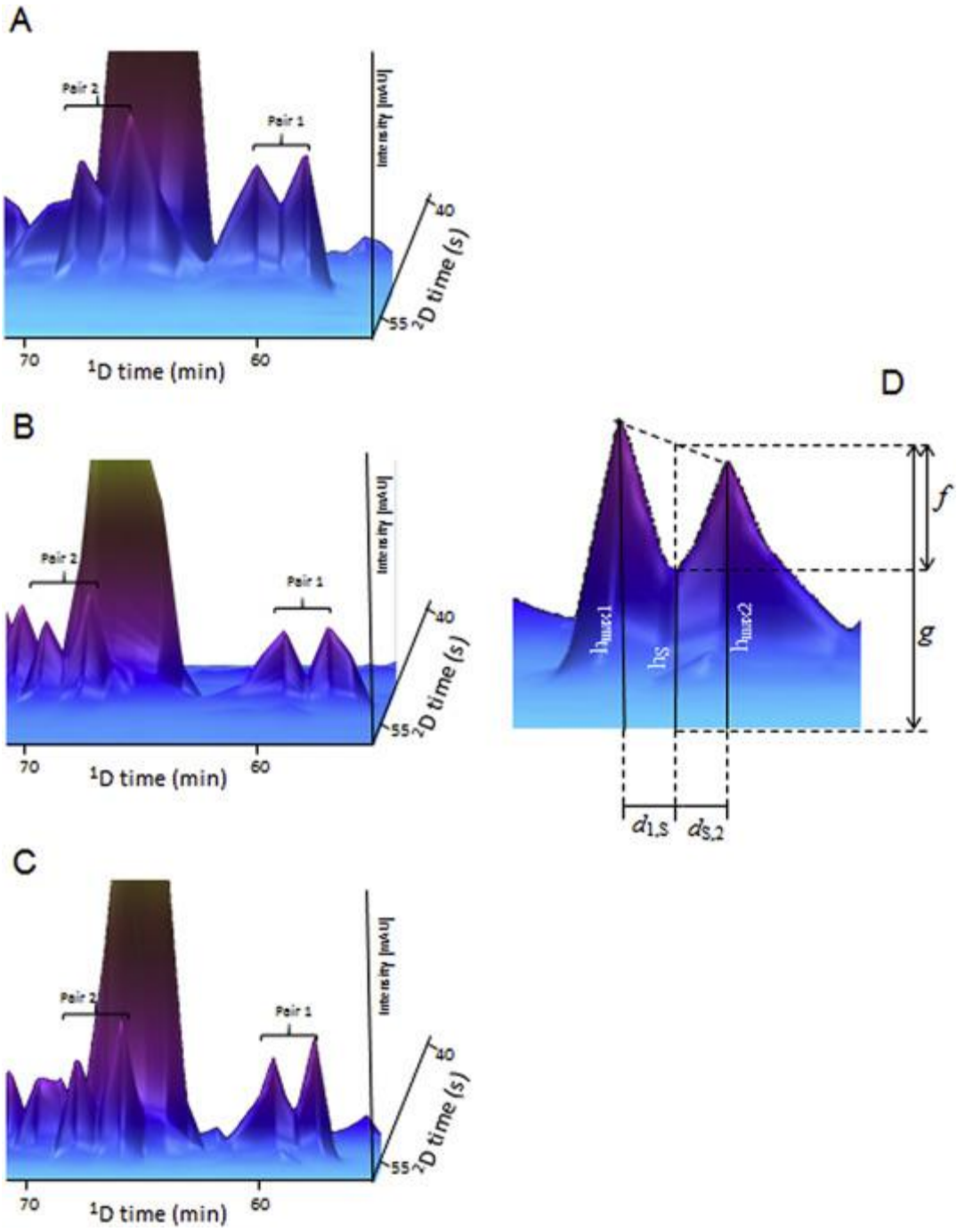

Fig. 4. Resolution obtained by using active modulation with phenyl-hexyl trapping columns of the two pairs of the studied peaks, using make-up flow rates equal to 5- (A), 7- (B) and 9-times (C) ^{1}D flow rate, and practical scheme of the calculation of the valley-to-peak ratio used for the estimation of resolution between critical pairs 1 and 2 (D).

3.4. Overall comparison

As already described in the previous sections, different approaches have been considered to further improve the separation capabilities of the initial HILIC × RP method directed towards the profiling of secondary metabolites in licorice. In general, the use of focusing modulation, either using trapping columns or active modulation, allowed a clear improvement on the separation of the complex metabolite profile of this sample (Fig. 1). In fact, these two approaches allowed obtaining good degrees of resolution between the studied pairs (Fig. 4 and Fig.S4). In general, better separations were obtained using trapping columns in forward elution mode and using active modulation with make-up

flow rates 9-times the ^{1}D flow rate. Although in both cases, the two stationary phases studied produced comparable performance, the phenyl-hexyl particles were slightly better than C_{18} particles. Under these conditions, similar orthogonality values as well as resolution between the critical pairs were obtained (Table 2, Table 3). However, practical peak capacities were significantly higher using active modulation (2131 vs 1811), and thus, this procedure resulted more favorable. The use of non-focusing modulation by sampling loops could only provide comparable performance in some aspects when modulation time was significantly reduced, thus, increasing ^{1}D sampling rate. However, due to very fast ^{2}D separations, the total 2D peak capacity attainable was severely compromised with respect to active modulation.

With the aim to further obtain more data illustrating the performance of each procedure, the attainable sensitivity under each separation conditions was studied by analyzing peak S (Fig. 5). Values of normalized sensitivity for each set-up are included in Table 1, Table 2, Table 3 This value was obtained by considering the sensitivity for peak S in the original method with respect to the sensitivity obtained in each case. As can be observed from those results, the set-up involving the use of active modulation using phenyl-hexyl traps and make-up flow at 9-time ^{1}D flow rate produced the highest sensitivity enhancement. Consequently, active modulation was shown again as the best possible alternative set-up for the profiling of secondary metabolites in licorice by HILIC × RP in order to further enhance both resolving power and sensitivity.

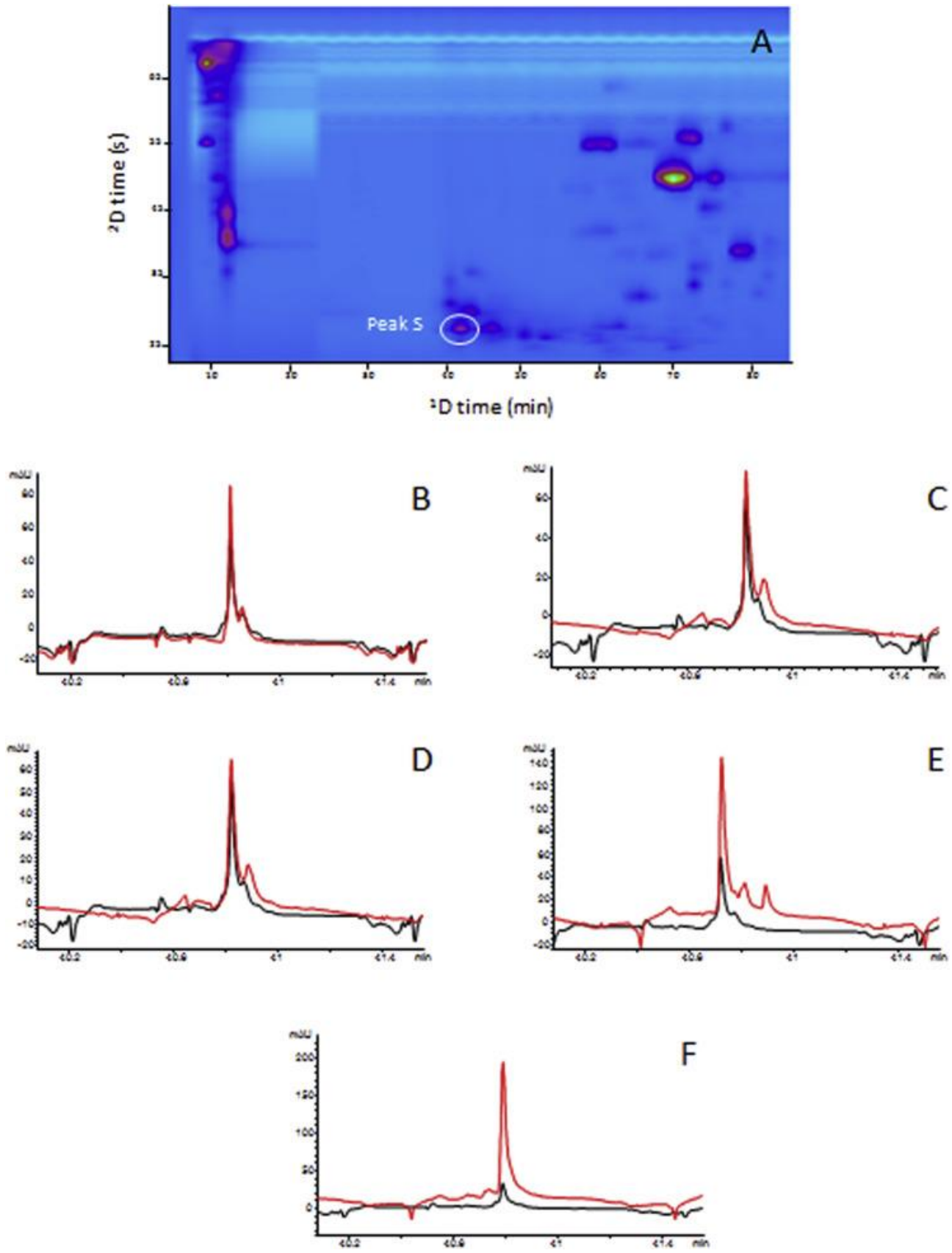

Fig. 5. Panel A: 2D-plot (254 nm) of the separation obtained in the original method. Sensitivity comparison (peak S) of the original method with the set-up of each modulation configuration using: B, 50 μL sampling loops in combination with 50 mm length column in the ^{2}D; C, 50 μL sampling loops in combination with 30 mm length column in the ^{2}D; D, C_{18} trapping columns with forward elution; E, active modulation with phenyl-hexyl traps and make-up flow rate equal to 9-times ^{1}D flow

rate, and; F, sensitivity gain with the 250 × 2,1 mm, 3,5 μm ^{1}D column. (Retention times of analyses with different ^{2}D gradient are aligned to help the comparison).

In this regard, theoretically, further sensitivity gains could be obtained if a column with higher sample loadability is used in ^{1}D. For this reason, a last attempt was made using the optimum separation conditions but increasing the ^{1}D column internal diameter to 2.1 mm. That column allowed an increase on the injection volume to 15 μL, although higher ^{1}D flow rates were also needed to maintain the ^{1}D separation. This would have a deleterious effect on the fraction volume transferred to ^{2}D, but considering that active modulation was employed with trapping columns, the fraction volume should not have such a critical influence on the coupling. As shown in Table S3, the normalized sensitivity obtained was further increased with respect to the use of the microbore ^{1}D column (Fig. 5F); however, the separation obtained was severely hampered, and the resolution between the critical pairs studied was completely lost (Table S3). Thus, this modification was not considered favorable, bearing in mind that compromises should be always taken between sensitivity, resolving power and overall peak capacity obtainable.

4. Conclusions

In the present contribution, different strategies are proposed and compared to further increase HILIC × RP method performance for the analysis of complex food samples, using licorice as a model sample. When using non-focusing modulation based on sampling loops, the use of very short columns (30 mm) in the ^{2}D was shown to be beneficial to increase performance, taking advantage of higher sampling loops volume to increase solvent dilution, thus, minimizing the deleterious effects due to solvent strength mismatch between HILIC and RP. However, the use of focusing modulation procedures was demonstrated to be able to increase not only resolving power but also peak capacity, reducing the effects of solvent mismatch at the same time that producing a focusing effect at the beginning of the ^{2}D analyses. In addition, significant sensitivity gains could be also obtained through the use of active modulation with a relatively high make-up flow rate. A total of 94 peaks were successfully separated in the set-up involving the use of active modulation with phenyl-hexyl trapping columns and a make-up flow rate 9-times higher than the corresponding ^{1}D flow rate, compared to the initial method (79 peaks), increasing sensitivity more than twice. In summary, the results obtained demonstrate the great applicability and potential that active modulation may have for the profiling of complex food samples by HILIC × RP.

Acknowledgements

The authors would like to thank Project AGL2014-53609-P (MINECO, Spain) for financial support.

Appendix A. Supplementary data

The following is the supplementary data related to this article:

Supplementary.

References

[1] P.Q. Tranchida, P. Donato, F. Cacciola, M. Beccaria, P. Dugo, L. Mondello**Potential of comprehensive chromatography in food analysis.** TrAC Trends Anal. Chem., 52 (2013), pp. 186-205

[2]M. Sarrut, G. Cretier, S. Heinisch**Theoretical and practical interest in UHPLC technology for 2D-LC.** TrAC Trends Anal. Chem., 63 (2014), pp. 104-112

[3] X. Shi, S. Wang, Q. Yang, X. Lu, G. Xu**Comprehensive two-dimensional chromatography for analyzing complex samples: recent new advances.** Anal. Methods, 6 (2014), pp. 7112-7123

[4] F. Bedani, P.J. Schoenmakers, H.G. Jansen**Theories to support method development in comprehensive two-dimensional liquid chromatography – a review.** J. Sep. Sci., 35 (2012), pp. 1697-1711
[5]F. Cacciola, S. Farnetti, P. Dugo, P.J. Marriott, L. Mondello**Comprehensive two-dimensional liquid chromatography for polyphenol analysis in foodstuffs.** J. Sep. Sci., 40 (2017), pp. 7-24
[6] M.J. Egeness, M.C. Breadmore, E.F. Hilder, R.A. Shellie**The modulator in comprehensive two-dimensional liquid chromatography.** LC-GC Eur., 5 (2016), pp. 268-276
[7]F. Cacciola, P. Donato, D. Giuffrida, G. Torre, P. Dugo, L. Mondello**Ultra high pressure in the second dimension of a comprehensive two-dimensional liquid chromatographic system for carotenoid separation in red chili peppers.** J. Chormatogr. A, 1255 (2012), pp. 244-251
[8]H. Tian, J. Xu, Y. Guan**Comprehensive two-dimensional liquid chromatography (NPLC x RPLC) with vacuum-evaporation interface.** J. Sep. Sci., 31 (2008), pp. 1677-1685
[9] M.E. Creese, M.J. Creese, J.P. Foley, H.J. Cortes, E.F. Hilder, R.A. Shellie, M.C. Breadmore**Longitudinal on-column thermal modulation for comprehensive two-dimensional liquid chromatography.** Anal. Chem., 89 (2017), pp. 1123-1130
[10]F. Cacciola, P. Jandera, E. Blahovà, L. Mondello**Development of different comprehensive two-dimensional systems for the separation of phenolic antioxidants.** J. Sep. Sci., 29 (2006), pp. 2500-2513
[11] R.J. Vonk, A.F.G. Gargano, E. Davydova, H.L. Dekker, S. Eeltink, L.J. de Koning, P.J. Schoenmakers**Comprehensive two-dimensional liquid chromatography with stationary-phase-assisted modulation coupled to high-resolution mass spectrometry applied to proteome analysis of *Saccharomyces cerevisiae.*** Anal. Chem., 87 (2015), pp. 5387-5394
[12]Y. Zhao, S.S.W. Szeto, R.P.W. Kong, C.H. Law, G. Li, Q. Qan, Z. Zhang, Y. Wang, I.K. Chu**Online two-dimensional porous graphitic carbon/reversed phase liquid chromatography platform applied to shotgun proteomics and glycoproteomics.** Anal. Chem., 86 (2014), pp. 12172-12719
[13]E. Sommella, O.H. Ismail, F. Pagano, G. Pepe, C. Ostacolo, G. Mazzoccanti, M. Russo, E. Novellino, F. Gasparrini, P. Campiglia**Development of an improved online comprehensive hydrophilic interaction chromatography × reversed-phase ultra-high-pressure liquid chromatography platform for complex multiclass polyphenolic sample analysis.** J. Sep. Sci., 40 (2017), pp. 2188-2197
[14]A.F. Gargano, M. Duffin, P. Navarro, P.J. Schoenmakers**Reducing dilution and analysis time in online comprehensive two-dimensional liquid chromatography by active modulation.** Anal. Chem., 88 (2016), pp. 1785-1793
[15]L. Montero, E. Ibañez, M. Russo, R. di Sanzo, L. Rastrelli, A.L. Piccinelli, R. Celano, A. Cifuentes, M. Herrero**Metabolite profiling of licorice (*Glycyrrhiza glabra*) from different locations using comprehensive two-dimensional liquid chromatography coupled to diode array and tandem mass spectrometry detection.** Anal. Chim. Acta, 913 (2016), pp. 145-159
[16]P. Montoro, M. Maldini, M. Russo, S. Postorino, S. Piacente, C. Pizza**Metabolic profiling of roots of liquorice (*Glycyrrhiza glabra*) from different geographical areas by ESI/MS/MS and determination of major metabolites by LC-ESI/MS and LC-ESI/MS/MS.** J. Pharm. Biomed. Anal., 54 (2011), pp. 535-544
[17] X. Li, D.R. Stoll, P.W. Carr**Equation for peak capacity estimation in two-dimensional liquid chromatography.** Anal. Chem., 81 (2009), pp. 845-850
[18] M.R. Schure, J.M. Davis**Orthogonal separations: comparison of orthogonalitymetrics by statistical analysis.** J. Chromatogr. A, 1414 (2015), pp. 60-76
[19] M. Camenzuli, P.J. Schoenmakers**A new measure of orthogonality for multi-dimensional chromatography.** Anal. Chim. Acta, 838 (2014), pp. 93-101
[20]S. Peters, G. Vivó-Truyols, P.J. Marriott, P.J. Schoenmakers**Development of a resolution metric for comprehensive two-dimensional chromatography.** J. Chromatogr. A, 1146 (2007), pp. 232-241

[21]P. Jandera, T. Hajek, P. Cesla**Effects of the gradient profile, sample volume and solvent on the separation in very fast gradients, with special attention to the second-dimension gradient in comprehensive two-dimensional liquid chromatography.** J. Chromatrogr. A, 1218 (2011), pp. 1995-2006
[22]F. Gritti, G. Guiochon**Theoretical investigation of diffusion along columns packed with fully and superficially porous particles.** J. Chromatogr. A, 1218 (2011), pp. 3476-3488
[23]R. Hayes, A. Ahmed, T. Edge, H. Zhang**Core–shell particles: preparation, fundamentals and applications in high performance liquid chromatography.** J. Chromatogr. A, 1357 (2014), pp. 36-52
[24]R.E. Murphy, M.R. Schure, J.P. Foley**Effect of sampling rate on resolution in comprehensive two-dimensional liquid chromatography.** Anal. Chem., 70 (1998), pp. 1585-1594
[25]F. Cacciola, P. Jandera, Z. Hajdù, P. Česla, L. Mondello**Comprehensive two-dimensional liquid chromatography with parallel gradients for separation of phenolic and flavone antioxidants.** J. Chromatogr. A, 1149 (2007), pp. 73-87

Table 1. Comprehensive two-dimensional method parameters applied to the profiling of secondary metabolites from licorice using non-focusing modulation.

		^{2}D - C_{18} 50 × 4.6 mm, 2.7 µm			^{2}D - C_{18} 30 × 4.6 mm, 2.7 µm		
	Sampling loop volume	**20 µL**	**30 µL**	**50 µL**	**20 µL**	**30 µL**	**50 µL**
^{1}D	L (mm)	150	150	150	150	150	150
	I.D. (mm)	1.0	1.0	1.0	1.0	1.0	1.0
	Particle size (µm)	3.5	3.5	3.5	3.5	3.5	3.5
	Flow rate (µL min^{-1})	15	15	15	15	15	15
(min)	2.69 2.69 2.69	2.47	2.47	2.47			
^1n_c	30 30 30	33	33	33			
<β>	1.33 1.33 1.33	1.25	1.25	1.25			
^1n_c corr.	23 23 23	27	27	27			
^{2}D							
(s)	1.06	0.90	0.78	1.02	1.00	1.00	
^2n_c	75	88	101	60	61	61	
LC × LC	Analysis time (min)	80	80	80	80	80	80
	t_s	1.93σ	1.93σ	1.93σ	1.62σ	1.62σ	1.62σ
	Modulation time (min)	1.3	1.3	1.3	1.0	1.0	1.0
	M – number of modulations	62	62	62	80	80	80
	$^2V_{inj}$ (V dilution)	20 µL (0.5 µL)	30 µL (10.5 µL)	50 µL (30.5 µL)	20 µL (5.0 µL)	30 µL (15.0 µL)	50 µL (35.0 µL)
	% ^{2}D column void volume	4%	6%	10%	7%	10%	17%
	Gradient delay volume (mL)	0.72	0.74	0.76	0.48	0.48	0.51
	^{2}D column operation preassure (bar)	299	295	298	187	185	190
	Z_1	0.84	0.91	0.92	0.89	0.82	0.85
	Z_2	0.97	0.96	0.99	0.97	0.98	0.97
	Z_-	0.69	0.77	0.81	0.91	0.89	0.86
	Z_+	0.83	0.87	0.84	0.99	0.95	0.99
	A_O	68%	76%	79%	82%	82%	84%
	Resolution pair 1	0.65	0.67	0.70	0.75	0.83	0.89
	Resolution pair 2	–	–	–	–	–	–
	Normalized sensitivity	0.85	1.00	1.37	1.08	1.32	1.61
	$^{2D}n_c$ theoretical	2250	2640	3030	1980	2013	2013
	$^{2D}n_c$ practical	1730	1964	2253	1706	1736	1780
	$^{2D}n_c$ corr.	1401	1493	1780	1399	1424	1495

<β>, average ^{1}D broadening factor; ^1n_c corr.: calculated according to eq. (2); t_s, sampling time; A_O, orthogonality; $^{2D}n_c$ theoretical: $^1n_c \times {}^2n_c$; $^{2D}n_c$ practical: calculated according to eq. (4); $^{2D}n_c$ corr.: $^{2D}\ n_c \times A_0$.

Table 2. Comprehensive two-dimensional method parameters applied to the profiling of secondary metabolites from licorice using trapping columns-based focusing modulation.

		Forward elution		Backflush elution	
	Trapping column	**C18**	**Phenyl-hexyl**	**C18**	**Phenyl-hexyl**
^{1}D	L (mm)	150	150	150	150
	I.D. (mm)	1.0	1.0	1.0	1.0
	Particle size (μm)	3.5	3.5	3.5	3.5
	Flow rate (μLmin^{-1})	15	15	15	15
(min)		2.11	2.11	2.11	2.11
$^{1}n_c$		39	39	39	39
<β>		1.32	1.32	1.32	1.32
$^{1}n_c$ corr.		30	30	30	30
^{2}D					
(s)		0.97		0.96	0.98	0.98	
$^{2}n_c$		63		64	62	62	
LC × LC	Analysis time (min)			80	80	80	80
	t_s			1.88σ	1.88σ	1.88σ	1.88 σ
	Modulation time (min)			1.0	1.0	1.0	1.0
	M – number of modulations			80	80	80	80
	Gradient delay volume (mL)			0.51	0.51	0.44	0.44
	^{2}D column operation preassure (bar)			260	258	253	254
	Z_1			0.94	0.86	0.83	0.87
	Z_2			0.92	0.94	0.97	0.93
	Z_-			0.94	0.89	0.92	0.97
	Z_+			0.93	0.98	0.92	0.83
	A_0			87%	84%	83%	81%
	Resolution pair 1			0.80	0.80	0.79	0.81
	Resolution pair 2			0.81	0.85	0.72	0.78
	Normalized sensitivity			1.15	0.99	0.59	0.75
	$^{2D}n_c$ theoretical			2457	2496	2418	2418
	$^{2D}n_c$ practical			1792	1811	1777	1777
	$^{2D}n_c$ corr.			1559	1521	1475	1439

<β>, average ^{1}D peak broadening factor; $^{1}n_c$ corr.: calculated according to eq. (2); t_s, sampling time; A_O, orthogonality; $^{2D}n_c$ theoretical: $^{1}n_c \times {}^{2}n_c$; $^{2D}n_c$ practical: calculated according to eq. (4); $^{2D}n_c$ corr.: $^{2D}n_c \times A_O$.

Table 3. Instrumental parameters employed and method performance descriptors from the use of active modulation for the profiling of secondary metabolites from licorice.

		C18 trapping columns			Phenyl-hexyl trapping columns		
	Make-up flow rate	**5 × ^{1}F**	**7 × ^{1}F**	**9 × ^{1}F**	**5 × ^{1}F**	**7 × ^{1}F**	**9 × ^{1}F**
^{1}D	L (mm)	150	150	150	150	150	150
	I.D. (mm)	1.0	1.0	1.0	1.0	1.0	1.0
	Particle size (μm)	3.5	3.5	3.5	3.5	3.5	3.5
	^{1}F (Flow rate, μL min^{-1})	15	15	15	15	15	15
(min)	2.11 2.11 2.11	2.11 2.11	2.11				
^1n_c	39 39 39	39 39	39				
<β>	1.33 1.33 1.33	1.32 1.32	1.32				
^1n_c corr.	29 29 29	30 30	30				
^{2}D							
(s)	0.93	0.84	0.81	0.96	0.84	0.81	
^2n_c	66	73	75	63	73	75	
	Analysis time (min)	80	80	80	80	80	80
	t_s	1.88σ	1.88σ	1.88σ	1.88σ	1.88σ	1.88σ
	Modulation time (min)	1.0	1.0	1.0	1.0	1.0	1.0
	M – number of modulations	80	80	80	80	80	80
	Gradient delay volume (mL)	0.49	0.49	0.49	0.49	0.49	0.49
	Column operation preassure (bar)	266	267	266	259	261	262
	Z_1	0.87	0.89	0.90	0.87	0.87	0.88
	Z_2	0.98	0.96	0.96	0.96	0.94	0.94
LC × LC	Z_-	0.91	0.92	0.91	0.87	0.89	0.89
	Z_+	0.93	0.93	0.94	0.96	0.97	0.95
	A_O	85%	86%	86%	84%	84%	84%
	Resolution pair 1	0.69	0.82	0.85	0.71	0.91	0.93
	Resolution pair 2	0.81	0.86	0.88	0.82	0.86	0.88
	Normalized sensitivity	1.46	1.59	1.98	0.91	1.67	2.01
	$^{2D}n_c$ theoretical	2574	2847	2925	2457	2847	2925
	$^{2D}n_c$ practical	1888	2075	2128	1806	2070	2131
	$^{2D}n_c$ corr.	1605	1785	1830	1517	1739	1790

<β>, average ^{1}D peak broadening factor; ^1n_c corr.: calculated according to eq. (2); t_s, sampling time; A_O, orthogonality; $^{2D}n_c$ theoretical: $^1n_c \times {}^2n_c$; $^{2D}n_c$ practical: calculated according to eq. (4); $^{2D}n_c$ corr.: $^{2D}\, n_c \times A_O$.

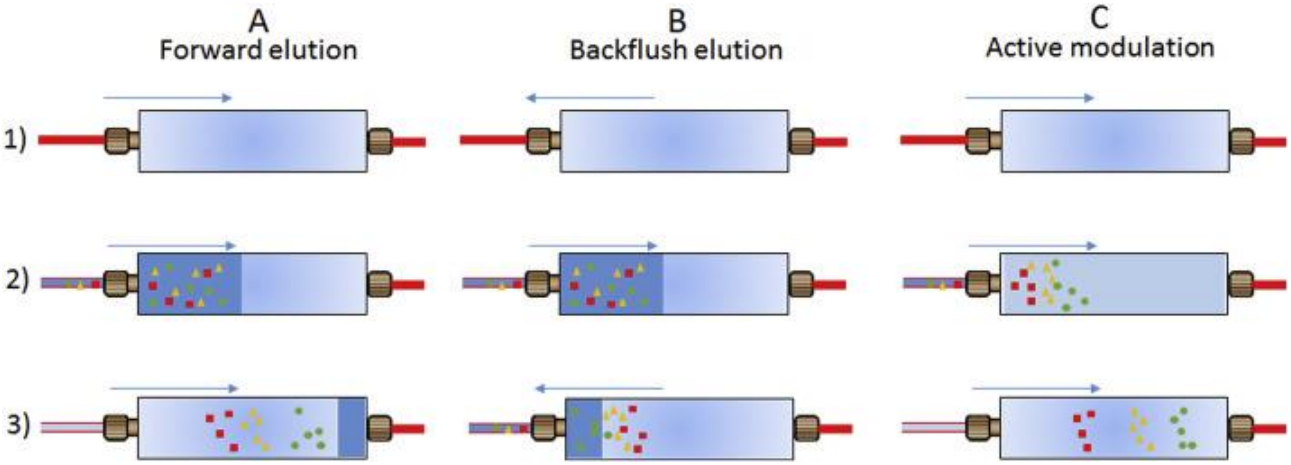

Fig. 3. Hypothetical scheme of the retention/elution of secondary metabolites from licorice into the trapping columns under forward elution mode (A), backflush elution mode (B), and active modulation (C) set-ups studied, following the procedure: 1) Trapping column filled with ^{2}D initial mobile phase (injection position, just after valve actuation); 2) Trapping column filled with ^{1}D effluent fraction (collection position) diluted in strong (A and B) or weak (C) solvent; 3) start of ^{2}D gradient. Arrows indicate flow direction.

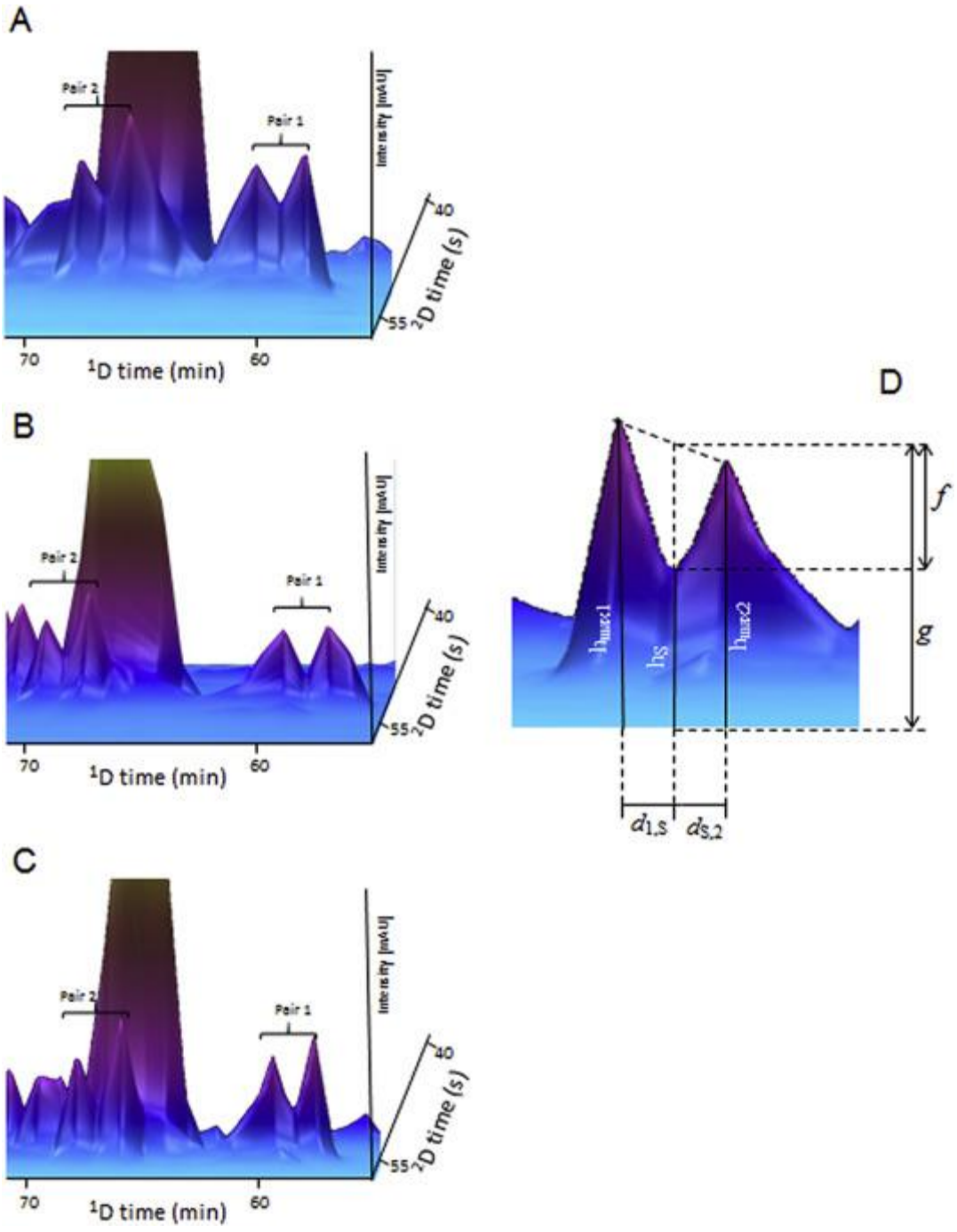

Fig. 4. Resolution obtained by using active modulation with phenyl-hexyl trapping columns of the two pairs of the studied peaks, using make-up flow rates equal to 5- (A), 7- (B) and 9-times (C) ^{1}D flow rate, and practical scheme of the calculation of the valley-to-peak ratio used for the estimation of resolution between critical pairs 1 and 2 (D).

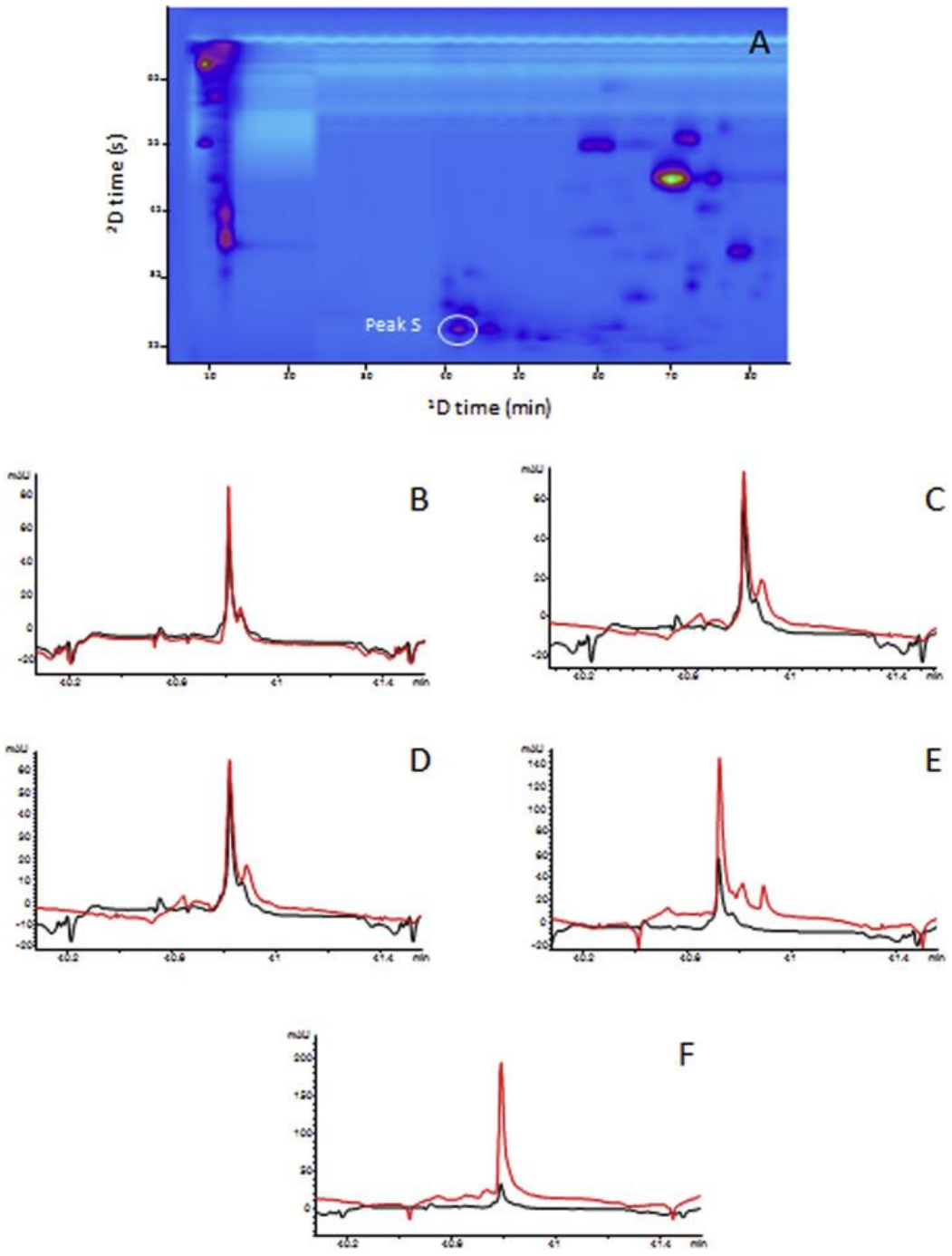

Fig. 5. Panel A: 2D-plot (254 nm) of the separation obtained in the original method. Sensitivity comparison (peak S) of the original method with the set-up of each modulation configuration using: B, 50 µL sampling loops in combination with 50 mm length column in the ^{2}D; C, 50 µL sampling loops in combination with 30 mm length column in the ^{2}D; D, C_{18} trapping columns with forward elution; E, active modulation with phenyl-hexyl traps and make-up flow rate equal to 9-times ^{1}D flow rate, and; F, sensitivity gain with the 250 × 2,1 mm, 3,5 µm ^{1}D column. (Retention times of analyses with different ^{2}D gradient are aligned to help the comparison).